ICEMS'2003

PROCEEDINGS OF THE SIXTH INTERNATIONAL CONFERENCE ON

ELECTRICAL MACHINES AND SYSTEMS

November 9-11, 2003, Beijing, China

Volume I

Edited by

Fangquan Rao Guobiao Gu

INTERNATIONAL ACADEMIC PUBLISHERS

WORLD PUBLISHING CORPORATION

III. Special Machines

An Improved 2-Phase Snail-Cam Type Fan Motor Design

Ji-Young Lee[1], Geun-Ho Lee[1], Jeong-Jong Lee[1], Jung-Pyo Hong[1], *Senior Members, IEEE*, and Kyung-Ho Ha[2]

[1]Dept. of Electrical Eng., Changwon Nat'l Univ., Changwon, Gyeongnam, Korea

[2]Electrical Steel Research Team of Technical Research Lab., POSCO, Gyeongbuk, Korea

Phone: 82-055-2625966 Fax: 82-055-2639956 E-mail: jyecad@korea.com Website: http://ecad.eecu.net

Abstract- **This paper deals with the design of a 2-phase Switched Reluctance Motor (SRM) used for the cooling fan motor of a refrigerator. To reduce the dead zone and improve the efficiency, the snail-cam type rotor pole and the asymmetric stator pole are investigated. For the optimal shape design, the performances of each model are obtained from numerical calculation results by 2D time-stepping finite element method (FEM) coupled with circuit equations. The accuracy of analysis is verified by comparing the analysis results with experimental data. As the results of investigation, an improved shape of stator and rotor poles are proposed.**

I. Introduction

Recently, the Brushless DC motor (BLDC) has been commonly used in household applications, but high cost of permanent magnets and complexity of the controllers are some of their disadvantages. Compared with the BLDC, the Switched Reluctance Motor (SRM) has many advantages such as solidity, low cost drive topology and economical efficiency due to simple construction [1]-[2]. These characteristics are competent to satisfy the demands for a part of household electric appliances.

This paper deals with the design of a 2-phase SRM, which is the cooling fan motor of a refrigerator. The structure of the prototype and its problems are introduced and the redesign methodology is described in detail. In the redesign process, a snail-cam type rotor and asymmetric stator poles are investigated to solve the problems. The design variables are the stator pole arc, the ratio of the stator pole arc, the existence of the dip and rotor slot depth.

For selecting the optimal pole shapes, the average torque and efficiency are calculated by using a hybrid method combining 2D finite element method (FEM) with the voltage equation. 2D solvers can be used effectively to optimize lamination geometry, however it cannot be expected to give accurate magnetization curves for SRM because of the significant influence of end effects [1]. In the case of SRM design, the drive characteristic is also important as well as the inductance profile. Therefore, the end effect and the dynamic state performances are calculated in consideration of its supply and the accuracy of computation is verified by comparing the result with the experimental data for the prototype motor.

As the results of the investigation, an improved asymmetric stator and snail-cam type rotor poles are proposed. Comparison of the torque characteristics of prototype and improved motor reveals that an asymmetric stator pole and a deeper slot depth of rotor eliminate dead zones and results in higher efficiency.

II. Analysis Model And Procedure

Fig. 1 shows the configuration of the original cooling fan SRM and its supply. This prototype motor has a wide dead zone and a low efficiency because it was designed in disregard of its supply state. The falling period of current is very short because of the switch-off voltage, which is over 5 times the switch-on voltage.

To solve the problems, the supply converter was redesigned first to asymmetric bridge converter. The supply is important to improve motor characteristics because longer falling period of current can improve the torque ripple, but it also can raise a reverse torque. Therefore the motor shapes are also changed in consideration of the converter. The motor variables are proposed as shown on Fig. 2. The redesign variables are stator pole arc, the ratio of stator pole arc, the

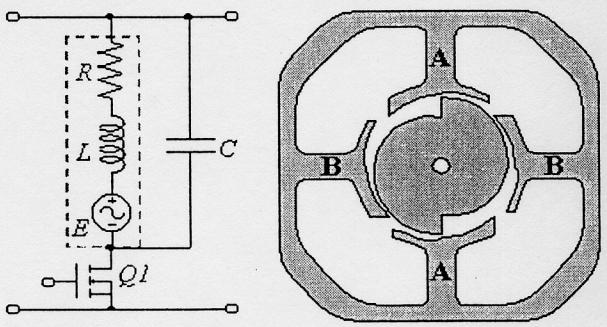

Fig. 1. Designed and fabricated drive (left) and prototype motor (right)

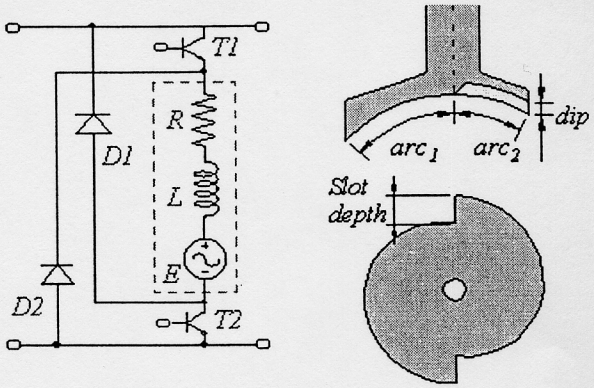

Fig. 2. Asymmetric bridge converter (left) and detail configurations (right)

existence of the dip and rotor slot depth as shown on right side of Fig. 2. The ratio of stator pole arc is the arc_1 versus arc_2. The arc_1 is longer side and the dip is on the other side, arc_2.

To improve the torque characters and efficiency, the variables are examined in 4 stages as follows:

1) Table I shows the initial combination of the variables. In this first stage, the switch turn-on angle is also considered because the switching angles influence current shape and magnetic characteristics of SRM. The base angle 0° is the position that stator and rotor poles are unaligned, and minus means the reverse direction to rotation. The big characters 'S' and 'A' mean symmetric and asymmetric pole shape, and the small characters 'a' and 'b' mean without and with dip, respectively. The number '10' and '20' is the absolute value of switch turn-on angle. Therefore, there are 8 type models in the first stage.

2) In the second stage, the existence of dip and the stator pole arc are decided for 8 type models selected in the first stage. The range of the stator pole arc is from 70° to 85° as shown in Table II. According to the general design equations in [1] and [2] the minimum stator pole arc is 90° in the case of 4-stator pole and 2-rotor pole SRM, but that is difficult to fabricate.

3) The ratio of stator pole arc is decided in the third stage. The ratio of symmetric stator pole is 1:1, and the ratios of asymmetric stator pole are the others as shown on Table II. The switch turn-on angle is still considered in this stage.

4) After the decision of stator pole shape and switch turn-on angle by stage 3, the rotor slot depth is selected in the last stage. The range of rotor slot depth is from 2 to 8mm as shown on Table II.

Fig. 3 presents an analysis procedure by 2D FEM to select optimal pole shapes. For the first time, the linear inductance profiles are calculated at constant current condition to find the exact unaligned position. And then, the magnetic performances of the models selected in each stage are calculated from the nonlinear dynamic analysis at constant voltage condition. This process helps to evaluate the different structure models and therefore, stator and rotor pole shapes can be decided to improve the motor efficiency and eliminate the dead zone.

TABLE I
CLASSIFICATION OF STATOR POLE SHAPES

Switch Turn- on Angle (°)	Symmetric Pole (arc_1: arc_2 = 1 : 1)		Asymmetric Pole (arc_1: arc_2 = 5 : 4)	
	without dip	with dip	without dip	with dip
-10	S10a	S10b	A10a	A10b
-20	S20a	S20b	A20a	A20b

TABLE II
RANGE OF VARIABLES

Stator Pole Arc (°)	70		75		80		85
Ratio of Stator Pole Arc	1 : 1		9 : 8		5 : 4		3 : 2
Rotor Slot Depth (mm)	2	3	4	5	6	7	8

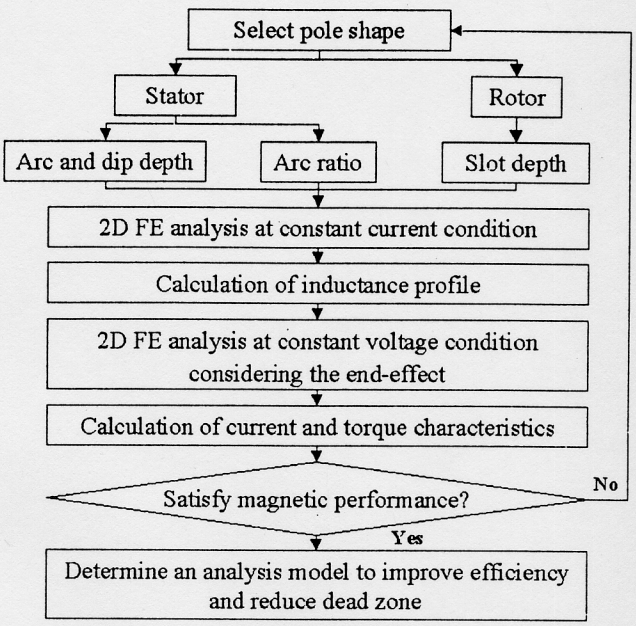

Fig. 3. Analysis procedure

III. ANALYSIS METHOD

A. Electromagnetic Analysis

The electro-magnetic governing equation of SRM with field variable $\boldsymbol{A}$ is obtained by Maxwell's electromagnetic equation as follows:

$$\nabla \times (\frac{1}{\mu} \nabla \times \boldsymbol{A}) = \boldsymbol{J}_0 \tag{1}$$

where $\boldsymbol{J}_0$ is the applied current density, $\boldsymbol{A}$ is the magnetic vector potential and μ is the magnetic permeability. For the analysis of the dynamic characteristics, voltage equation is coupled with (1) and then system matrix is obtained by time difference schemes. The method of the Maxwell stress tensor is used to calculate the static torque for the range of rotor position and phase excitation. Thus static torque is expressed according to the following (2).

$$\boldsymbol{T} = \oint_s \boldsymbol{r} \times \boldsymbol{P} \, d\boldsymbol{S} \tag{2}$$

where $\boldsymbol{r}$ is the distance vector of a point to axis rotation. Equation (2) is obtained by the surface integration of a stress tensor vector $\boldsymbol{P}$ over an air gap enclosing the rotor surface $\boldsymbol{S}$. The Maxwell stress tensor is given by (3)[3].

$$\boldsymbol{P} = \frac{1}{\mu_0}(\boldsymbol{n} \cdot \boldsymbol{B})\,\boldsymbol{B} - \frac{1}{2\mu_0}\boldsymbol{B}^2\boldsymbol{n} \tag{3}$$

where μ_0 is the permeability of free space, $\boldsymbol{n}$ is the normal vector to the surface $\boldsymbol{S}$, $\boldsymbol{B}$ is the magnetic flux density.

B. End Effect Calculation

From the electromagnetic analysis by 2D FEM, the linkage flux is calculated by difference between vector potentials at the both sides of an excited coil. Inductance is obtained by the ratio of the linkage flux and exciting current [4], but the results are not

accurate because the consideration of axial fringing effect is impossible in 2D FEM. For considering the end coil effect, empirical formulations should be developed by the equations in [5], [6] and [7]. In this paper, the end effect for the unaligned and aligned inductance is calculated by the equation in [7].

IV. Design And Analysis Results

A. Analysis and Measurement of Prototype

The comparison of measured and calculated inductance for prototype motor is shown in Table III. The error between the two inductances is under 5%. Fig. 4 shows the currents and torque of the machine. The current is obtained by experiment, and these results are compared with those of the analysis by FEM. Since the currents aspects coincide, the torque can be expected as shown in the lower part of Fig. 4. The efficiency of this motor is about 52.6%, but the dead zone is 16°.

B. Inductance Profiles

Fig. 5 shows the linear inductances of each analysis model, which consists of the variables on Table II and I. In this figure, the rotor positions are not absolute, and the start point (0°) is where the inductance is the minimum. The profiles are different from each other with respect to stator pole arc and the existence of dip, but they are same for the symmetric and asymmetric pole shapes because the saturation is neglected in the magnetic materials. The wider pole arc makes the longer increase span and the dip makes the sharp drop in the decrease span.

C. Stator and Rotor Pole Design

Fig. 6 shows the comparison of the effective minimum torque (EMT) and the efficiency of the models on Table I with respect to the stator pole arc on Table II. The EMT is the ratio of minimum torque to average torque. When this value is greater than zero, there is no dead zone, and the relative magnitude makes comparison of torque ripple of each model possible. In the most cases, the existence of dip and smaller stator pole arc makes higher EMT and lower efficiency.

Fig. 7 shows the results of analysis for the ratio of stator pole arc when the stator pole arc is 80° without dip. The EMT and the efficiency depend on the ratio of the stator pole and the switch turn-on angle. The highest efficiency is obtained when the ratio is 5:4 and switch turn-on angle is –10°. The EMT of this pole shape is also greater than zero.

After the decision of stator pole shape and switch turn-on angle, the rotor slot depth is selected for the last stage. Fig. 8 shows the average torque, the EMT and the efficiency with rotor slot depth. All performances increase until the rotor slot depth is 6mm.

From the above investigation, the SRM for the cooling fan is redesigned. The configuration and the performances are numerically compared with the prototype on Table IV. The efficiency is increased by 2.1% and dead zone is eliminated. The torque profile of redesigned motors is on Fig. 9 and this is graphically compared with Fig. 4.

TABLE III
COMPARISON OF MEASURED AND CALCULATED INDUCTANCES

	Measured Inductance (mH)	Calculated Inductance (mH)			Error (%)
		2D FEM	End Effect	Sum	
Aligned	173.18	169.07	12.41	181.48	4.79
Unaligned	79.78	50.86	27.01	77.87	2.39

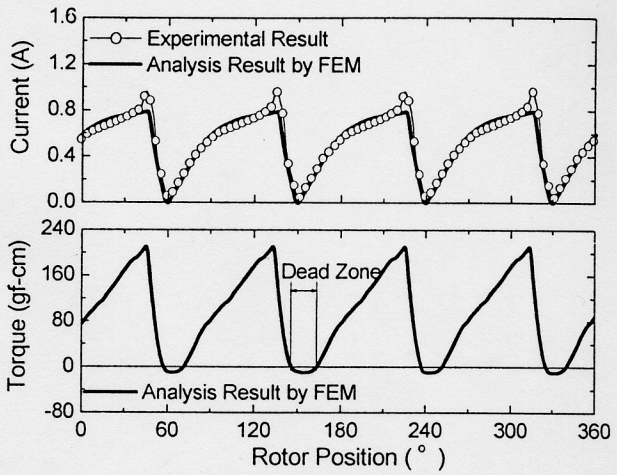

Fig. 4. Current (upper) and torque (lower) of prototype

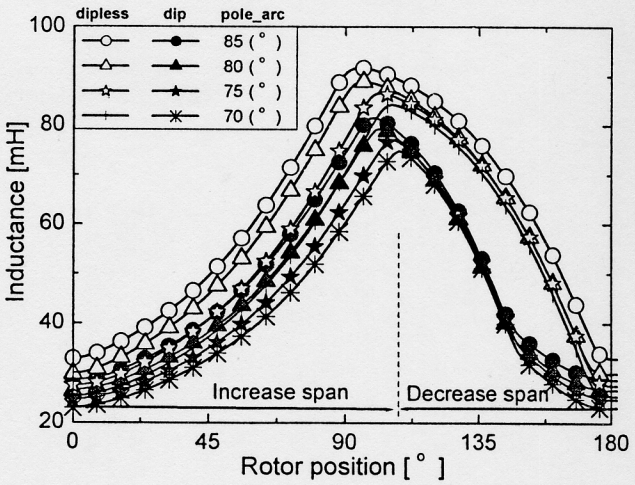

Fig. 5. Inductance profiles of symmetric stator pole without dip, and symmetric stator pole with dip for rotor position and stator pole arc

TABLE IV
COMPARISON OF PROTOTYPE AND IMPROVED MODEL

	Prototype	Improved Model
Stator Pole Arc (°)	85	80
Ratio of Stator Pole Arc	9 : 8	5 : 4
Existence of Dip	Yes	No
Rotor Slot Depth (mm)	4	6
Average Torque (kgf-cm)	79.6	83.0
Efficiency (%)	52.6	54.7
Dead Zone (°)	16	0

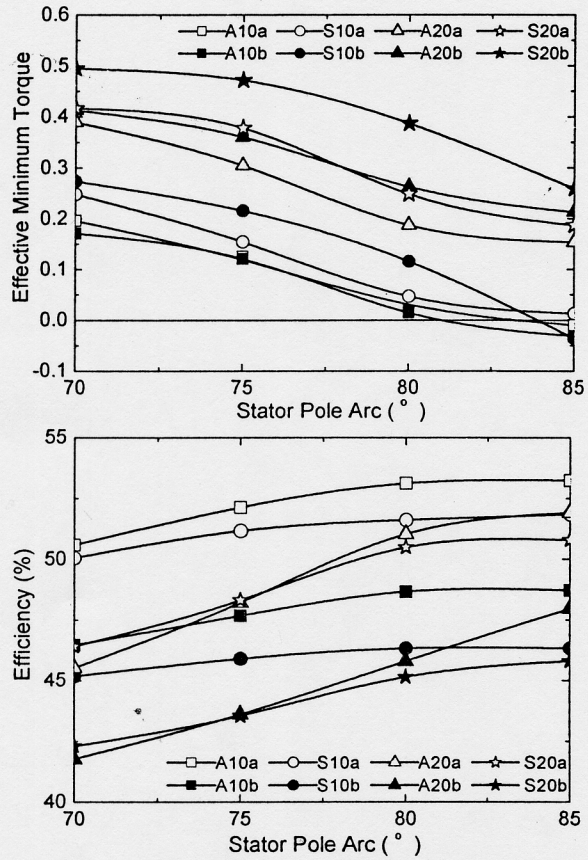

Fig. 6. Effective minimum torque (upper) and efficiency (lower) with respect to stator pole arc

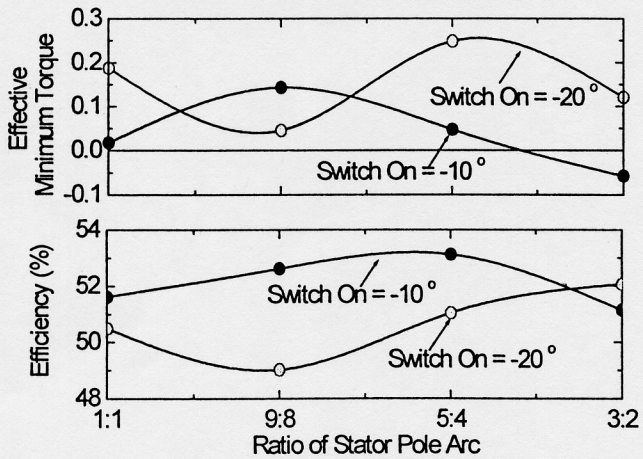

Fig. 7. Effective minimum torque (upper) and efficiency (lower) with respect to the ratio of stator pole arc

V. CONCLUSIONS

This paper demonstrates the effect of stator and rotor pole shapes on torque characteristics for 2-phase SRM. The detail trends of the performance according to various design parameters are investigated by 2D time stepping FEM coupled with voltage equation. As the redesigned results show, the improved motor has a asymmetric stator pole and a snail-cam rotor with deeper slot depth. The efficiency of the redesigned motor is higher than that of the original prototype and the dead zone is completely eliminated.

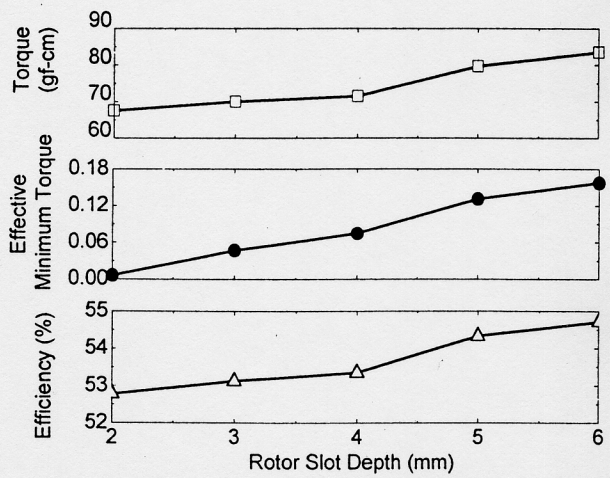

Fig. 8. Average torque (upper), effective minimum torque (middle) and efficiency (lower) with respect to the rotor slot depth

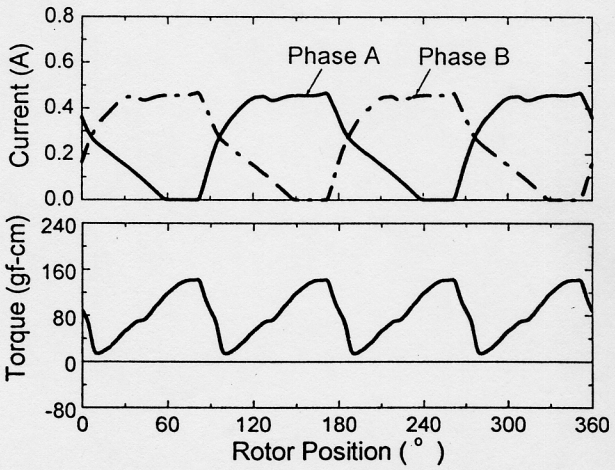

Fig. 9. Current (upper) and torque (lower) of improved model

REFERENCES

[1] T. J. E. Miller, *Switched Reluctance Motors and Their Control*, Magna physics publishing and Clarendon Press Oxford, 1993.

[2] P. J. Lawrenson and el. "Variable-speed switched reluctance motors," *IEE Proceeding*, vol. 127, pp. 253-265, July, 1980

[3] M. J. DeBortoli and S. J. Salon, "Computation of forces and torque in electromagnetic devices using the finite element method," *International Conference on Electrical Machines*, pp. 699-705, August, 1990

[4] Koichi Koibuchi and el, "A basic study for optimal design of switched reluctance motor by finite element method," *IEEE Trans. on Magnetics*, vol. 33, pp. 2077-2080, March, 1997

[5] J. Corda and J. M. Stephenson, "Analytical estimation of the minimum and maximum inductances of a double-salient motor," *in Proceedings of the International Conference on Stepping Motors and Systems*, Lees, U. K., pp.50-59, September, 1979

[6] Yifan Tang, "Characterization, numerical analysis, and design of switched reluctance motors," *IEEE Trans. on Industry Application*, vol. 33, pp. 1544-1552, November/December, 1997.

[7] *User's Manual of PC-SRD VERSION 7.0*, SPEED CONSORTIUM, 1999